LC-TH-2000-055
DESY 00-178

Physics Opportunities with Polarized e^- and e^+ Beams at TESLA

Gudrid Moortgat-Pick[a1], Herbert Steiner[b2]

[a] DESY, Deutsches Elektronen–Synchrotron, D–22603 Hamburg, Germany
[b] Department of Physics and Lawrence Berkeley National Laboratory, University of California, Berkeley, CA 94720, USA

Abstract

Beam polarization at e^+–e^- linear colliders will be a powerful tool for high precision analyses. Often it is assumed that the full information from polarization effects is provided by polarization of the electron beam and no further information can be obtained by the simultaneous polarization of the positrons. In this paper we point out the advantages of polarizing both beams, and summarize the polarization-related results of the Higgs, Electroweak, QCD, SUSY and Alternative Theories working groups of the ECFA/DESY workshop for a planned linear collider operating in the energy range $\sqrt{s} = 500 - 800$ GeV.

[1]e-mail: gudrid@mail.desy.de
[2]e-mail: steiner@lbl.gov

1 Introduction

Physics beyond the Standard Model (SM) has a good chance to be discovered at the run II of Tevatron, which starts in March 2001, or at the LHC whose start is planned for 2006. However, it is well known that a Linear Collider (LC) will be needed for precise measurements and for the detailed exploration of possible New Physics (NP). It will also provide access to large uncharted regions of the parameter space of Grand Unified Theories (GUT). Furthermore a LC will make possible measurements of the SM with unprecedented precision. The main advantages of an e^-e^+ collider are the clear signatures that make possible precise measurements of the masses and couplings of the interacting particles. Moreover the chiral character of the couplings can be worked out at a LC by using beam polarization. The importance of such measurements and the physics accessible with polarized electrons has been discussed for example in reference [1].

In the limit of vanishing electron mass SM processes are initiated by electrons and positrons polarized in the same direction, i.e. $e^+_L e^-_R$ (LR) or $e^+_R e^-_L$ (RL), where the first (second) entries denote helicities or chiralities of corresponding particle. This follows from either the vector nature of γ or Z couplings or from the chiral structure of W interactions (helicity–conservation). For these processes positron polarization provides no fundamentally new information, but as we will indicate below it can, nevertheless, have important consequences [2]. In theories beyond the SM interactions involving (LL) and (RR) configuations are also allowed, and in this case the polarization of both beams offers a powerful tool for enhancing rates and suppressing SM backgrounds.

Within the framework of the ECFA/DESY Study for a Linear Collider in the TeV range studies were made of the physics consequences when both the electron and positron beams are polarized. The results show that there are five principal advantages to be gained when both beams are polarized: (1) higher effective polarization, (2) suppression of background (3) enhancement of luminosity (4) increased sensitivity to non-standard couplings, and (5) improved accuracy in measuring the polarization. These features will be discussed in greater detail in the following sections, where the polarization-related results of the individual physics working groups are summarized. Before doing so, however, we briefly indicate in Section 2 the experimental possibilities to produce and measure polarization at the LC. In Section 3 we present the results of the different working groups. The advantages that might be realized with positron polarization are summarized in tabular form in Section 4.

2 Production, Manipulation and Measurement of Polarized Beams at a LC

During its last year of running the SLC at SLAC had an average longitudinal electron beam polarization $P_{e^-} = 77\%$, and polarimetry was developed that allowed the polarization to be determined to better than 0.5% [2]. Polarization reversals could be made as desired on a pulse by pulse basis by reversing the handedness of the circular polarization of the laser used to photo-produce the electrons. Polarization rotators had to be used to prevent depolarization effects in the damping rings. Very similar techniques are applicable to LCs more generally, and $P_{e^-} \geq 80\%$ polarized electron beams together with polarimetry at the $\leq 0.5\%$ level should be possible.

Positron polarization, on the other hand, is intrinsically harder. The method of choice was originally suggested by Balakin and Mikhailichenko [3], who proposed to pair-produce longitudinally polarized positrons and electrons by circularly polarized photons generated by an electron beam in a helical undulator. At TESLA highly polarized ~ 20 MeV photons generated by 250 GeV electrons passing through a ~ 100 meter-long helical undulator could be used to produce the polarized positrons in a thin foil. Positron polarizations of $40 - 45\%$ are possible with no loss of luminosity. Higher polarization could be achieved in principle at the price of reduced intensity (e.g., $P_{e^+} = 55\%$ at $\sim 60\%$ of full intensity [4]). Reversing the sign of the polarization is much more difficult in this case. A possible way of making reasonably rapid spin reversals might be to use a pulsed magnet to steer the positrons into one (or the other) of two separate beam lines, each with its own set of solenoidal spin rotators, prior to injecting them into the damping rings [4]. No matter what method is used, however, care must be taken not to introduce systematic effects in the process of flipping the spin.

Polarimeters based on both Moeller and Compton scattering have been used to measure electron polarization. The highest analyzing power, and thus the greatest precision ($< 0.5\%$), has been attained by detecting the recoil electrons when circularly polarized laser photons Compton scatter from longitudinally polarized electrons. Detection of the scattered photons has also been used, but the analyzing power is much smaller and the precision is not as high. Polarimetry using Moeller scattering has the lowest analyzing power but it has been used to make measurements at the few percent level. Compton scattering is the same for electrons and positrons, so that the same polarimeters can be used for both.

When both beams are polarized a scheme developed by Blondel obviates the need for precision polarimetry. In this case measurement of the cross sections of all spin combinations ((RR), (RL), (LR), and (LL)) can be used to determine the effective polarization. It has the additional advantage that the polarization measured in this way is the luminosity-weighted value at the interaction point, rather than the value at the location of the polarimeter. With this scheme it is important that any differences in polarization between left- and right-handed electrons (or positrons) be carefully measured. To this end polarimetry will still be needed.

3 Results of Polarization Studies for a LC

Five working groups – Higgs, Electroweak Theory, QCD, Supersymmetry (SUSY) and Alternative Theories – worked out the physics potential of a planned linear collider with a first phase of $\sqrt{s} = 500 - 800$ GeV, which complements and extends the capabilities of the LHC. In particular the LC provides a well–defined initial state and allows the exploitation of the effects of polarizing the incoming beams.

3.1 Higgs Working Group

If a Higgs particle exists in Nature, the accurate study of its production and decay properties can be performed in the clean environment of e^+e^- linear colliders in order to establish experimentally the Higgs mechanism as the mechanism of electroweak symmetry breaking [5]. The study of Higgs particles will therefore represent a central theme of the TESLA physics programme.

3.1.1 Separation of production processes

Higgs production at a LC occurs mainly via WW fusion, $e^+e^- \to H\nu\bar{\nu}$, and Higgsstrahlung $e^+e^- \to HZ$. Polarizing both beams suitably enhances the signal and suppresses background. In Table 2 the scaling factors, i.e. ratios of polarized and unpolarized cross section, are compared for two cases (1) $P_{e^-} = \pm 80\%$ and (2) $P_{e^-} = \pm 80\%$, $P_{e^+} = \mp 60\%$ [6]. Here, and in all the subsequent sections of this paper, we will use the convention that + ($-$) polarization corresponds to R (L) chirality with helicity $\lambda = +\frac{1}{2}$ ($\lambda = -\frac{1}{2}$) for both electrons and positrons.

If a light Higgs with $m_H \leq 130$ GeV is assumed, which is the prefered range both by fits of precision observables in the SM [7] and also by predictions of SUSY theories (see e.g. [8]), Higgsstrahlung dominates for $\sqrt{s} \lesssim 500$ GeV and WW fusion for $\sqrt{s} \gtrsim 500$ GeV. At a LC with $\sqrt{s} =$ 500 GeV and unpolarized beams the two processes have comparable cross sections. Beam polarization can be used to enhance the WW–Fusion signal with respect to the HZ contribution by a factor 1.6 (1.7) if electron (electron and positron) beam polarization is available (see Table 2). Further, variation of the relative amounts of Higgs-strahlung and WW fusion makes it possible to keep the systematics arising from the contributions to the fitted spectrum for these two processes smaller than the statistical accuracy.

3.1.2 Suppression of background

Beam polarization is very effective for background suppression. With right-handed electron polarization WW and single Z background can be strongly suppressed. The latter is only important at high s. With simultaneous polarization of e^- and e^+ one gains another factor of about 2 in background suppression. Background from ZZ is slightly suppressed with (R0) but not with (RL). To separate the Higgsstrahlung process from WW fusion right-polarized electron configurations are very suitable. Simultaneous left-handed polarized positrons suppress WW fusion and WW background, but enhance the ZZ background. Even in the case when the signal to background ratio, S/B, improves only slightly by simultaneous polarization of the e^- and e^+ beams one gets an improvement in $S/\sqrt{B}$ of about 20% in (Table 2). Polarization of the positron beams is a powerful tool to suppress the single W background, $e^+e^- \to W^-e^+\nu$ and $e^+e^- \to W^+e^-\bar{\nu}$.

3.1.3 Determination of general $ZZ\Phi$ and $Z\gamma\Phi$ couplings

In an effective Lagrangian approach the general coupling between Z–, Vector– and Higgsboson can be written [9]:

$$\begin{aligned}\mathcal{L} &= (1+a_Z)\frac{g_Z m_Z}{2} H Z_\mu Z^\mu + \frac{g_Z}{m_Z}\sum_{V=Z,\gamma}[b_V H Z_{\mu\nu}V^{\mu\nu} \\ &\quad + c_V(\partial_\mu H Z_\nu - \partial_\nu H Z_\mu)V^{\mu\nu} + \tilde{b}_V H Z_{\mu\nu}\tilde{V}^{\mu\nu}], \end{aligned} \tag{1}$$

with $V_{\mu\nu} = \partial_\mu V_\nu - \partial_\nu V_\mu$, $\tilde{V}_{\mu\nu} = \epsilon_{\mu\nu\alpha\beta}V^{\alpha\beta}$.

Using, for example, the optimal–observable method [10] it is possible at a LC to determine the seven complex Higgs couplings with high accuracy: the CP–even a_Z, b_Z, c_Z and b_γ, c_γ and the CP–odd $\tilde{b}_Z$ and $\tilde{b}_\gamma$. Simultaneous beam polarization considerably improves the accuracy. In [9] a study was made for $\sqrt{s} = 500$ GeV and $\mathcal{L} = 300$ fb^{-1}. It compares the so–called optimal errors when tagging efficiences $\epsilon_\tau = 50\%$, $\epsilon_b = 60\%$ and beam polarization $P_{e^-} = 80\%$ and $P_{e^+} = 60\%$ are assumed. It shows that the $ZZ\Phi$ coupling is rather well constrained. However, to fix the $Z\gamma\Phi$ coupling beam polarization is essential. In Table 3 the optimal errors are listed for the three cases (1) $P_{e^-} = 0 = P_{e^+}$, (2) $P_{e^-} = 80\%$, $P_{e^+} = 0$ and (3) $P_{e^-} = 80\%$, $P_{e^+} = 60\%$. For this comparison we list the values for $\epsilon_\tau = 0\% = \epsilon_b$. It is obvious that beam polarization is a decisive tool to fix the general Higgs coupling. Simultaneous beam polarization of e^- and e^+ beams results in an further reduction of 20%–30% in the optimal errors compared to the case with $P_{e^-} = 80\%$ and unpolarized positrons.

3.2 Electroweak Working Group

At a LC it is possible to test the SM with unprecedented accuracy. At high $\sqrt{s}$ studies determining the triple gauge couplings [11, 12] and at low $\sqrt{s}$ an order–of–magnitude improvement in the accuracy of the determination of $\sin^2\Theta^l_{eff}$ at $\sqrt{s} = m_Z$ may well be possible [11, 13]. These measurements are based on the use of polarized beams. To achieve the high precision it will be necessary to determine the polarization of both beams with very high accuracy. The Blondel Scheme [11, 14] coupled with Compton polarimetry offers a promising method to realize these goals.

3.2.1 High $\sqrt{s}$

The production $e^+e^- \to W^+W^-$ occurs in lowest order via γ–, Z– and ν_e–exchange. In order to test the SM with high precision one can carefully study triple gauge boson couplings, which are generally parametrized in an effective Lagrangian by the C–, P–conserving couplings g_1^V, κ_V, λ_V and the C– or P– violating couplings g_4^V, g_5^V, $\tilde{\kappa}_V$ and $\tilde{\lambda}_V$ with $V = \gamma, Z$ [15]. In the SM at tree level the couplings have to be $g_1^V = 1 = \kappa_V$, while all other are identical to zero.

These couplings can be determined by measuring the angular distribution and polarization of the $W^\pm$'s. Simultaneously fitting of all couplings results in a strong correlation between the $\gamma-$ and $Z-$couplings whereas polarized beams are well suited to separate these couplings [11, 12].

If the polarization is only known up to $\Delta P_{e^-} \sim 1\%$ the statistical error in the gauge couplings would be smaller than the error due to the uncertainty in determining the beam polarization. With Compton polarimetry $\Delta P_{e^-} < 0.5\%$ should be possible. However, to reduce the errors further it is necessary to make $\Delta P_{e^-} \ll 1\%$. This can be done by different schemes, e.g. by measuring the polarization via the A_{LR} in the forward peak which is dominated by the $\tilde{\nu}$ exchange in the t–channel and has to be essentially one in this region, independent of anomalous gauge couplings. Another possibility is to use simultaneously polarized e^+ and e^- beams and thereby to reduce the error in a polarization measurement by a factor three to four [11]. The polarization can also be measured by using the Blondel Scheme, i.e. measuring the configurations (LR), (RL), (LL), and (RR) with high accuracy. A further advantage of using polarized e^- and e^+ beams is that one could gain about a factor 2 in running time.

It is well known that TESLA with its high luminosity is a very promising device to measure these couplings with high precision [11]. At $\sqrt{s} = 500$ GeV and with $|P_{e^-}| = 80\%$ statistical errors of about $\Delta\kappa_\gamma \leq 3 \times 10^{-4}$ and $\Delta\lambda_\gamma \leq 5 \times 10^{-4}$ can be reached. Moreover, using simultaneous beam polarization of $P_{e^-} = 80\%$ and $P_{e^+} = 60\%$ the errors can be further reduced by up to a factor 1.8 compared to the case with $P_{e^-} = 80\%$ and unpolarized positrons. [12] (see Table 4).

3.2.2 GigaZ

GigaZ refers to running TESLA at the Z resonance with to about 10^9 Z events. Beam polarization of both e^- and e^+ at GigaZ would make possible the most sensitive test of the SM ever made. The potential of this high–precision measurement for testing higher order quantum effects in the electroweak SM and its supersymmetric extensions has been studied in [13]. Polarizing both beams has the double advantage of increasing the effective polarization and significantly reducing the polarization error.

In the SM the left–right asymmetry A_{LR} depends only on the effective leptonic weak mixing angle:

$$A_{LR} = \frac{2(1 - 4\sin^2\Theta^l_{eff})}{1 + (1 - 4\sin^2\Theta^l_{eff})^2}. \tag{2}$$

The value of the weak mixing angle listed in the 2001 PDG Tables is $\sin^2\theta_{eff} = 0.23147(16)$ which corresponds to $A_{LR} \sim 0.15$. In this case the error on $\sin^2\theta_{eff}$ is about a factor of 8 smaller than the error on A_{LR}, i.e.

$$\delta(\sin^2\theta_{eff}) \sim \delta(A_{LR})/8. \tag{3}$$

The error on A_{LR} can be written

$$(\delta(A_{LR}))^2 = (\delta(A_{LR}(pol)))^2 + (\delta(A_{LR}(stat)))^2 \tag{4}$$

with

$$\delta(A_{LR}(pol)) = (A_{LR}/P_{eff})\delta(P_{eff}), \tag{5}$$

where the effective polarization is given by

$$P_{eff} = (P_{e^-} - P_{e^+})/(1 - P_{e^-}P_{e^+}). \tag{6}$$

From (6) and (4) we see that when $P_{e^-} = \pm 80\%$ and $P_{e^+} = \mp 40\%$, the effective polarization is increased from 80% to 91%, and even more important, the polarization uncertainty, $\delta(P_{eff})$ is reduced by a factor of 2 compared to the value obtained when only the electron beam is polarized. The values of both P_{eff} and $\delta(P_{eff})$ continue to improve as the positron polarization increases.

The statistical power of the data sample can be fully exploited only when $\delta(A_{LR}(pol)) < \delta(A_{LR}(stat))$. For $10^8 - 10^9$ Z's this occurs when $\delta(P_{eff}) < 0.1\%$. In this limit $\delta(\sin^2\theta_{eff}) \sim 10^{-5}$, which is an order–of–magnitude smaller than the present value of this error. Thus it will be crucial to minimize the error in the determination of the polarization. Improvements in Compton polarimetry might reduce the present error of 0.5% by a factor of two, but it is unlikely that 0.1% can be achieved. The desired precision should, nevertheless, be attainable with the Blondel Scheme, where it is not necessary to know the beam polarization with such extreme accuracy, since A_{LR} can be directly expressed via cross sections for producing Z's with longitudinally polarized beams:

$$\sigma = \sigma_{unpol}[1 - P_{e^-}P_{e^+} + A_{LR}(P_{e^+} - P_{e^-})], \tag{7}$$

$$A_{LR} = \sqrt{\frac{(\sigma^{RR} + \sigma^{RL} - \sigma^{LR} - \sigma^{LL})(-\sigma^{RR} + \sigma^{RL} - \sigma^{LR} + \sigma^{LL})}{(\sigma^{RR} + \sigma^{RL} + \sigma^{LR} + \sigma^{LL})(-\sigma^{RR} + \sigma^{RL} + \sigma^{LR} - \sigma^{LL})}}. \tag{8}$$

In this formula the absolute polarisation values of the left- and the right-handed states are assumed to be the same. Corrections have to be determined experimentally by means of polarimetry techniques; however, only relative measurements are needed, so that the absolute calibration of the polarimeter cancels [11]. Polarimetry is also needed to track the time dependence of the polarisation which could affect the attainable precision in this scheme.

As can be seen from (8) the Blondel scheme also requires some luminosity for the less favoured combinations (LL, RR). However only 10% of running time is needed for these combinations to reach the desired accuracy for these high precision measurements. Fig. 1 shows the statistical error on A_{LR} as a function of the positron polarisation for $P_{e^-} = 80\%$. Already with 20% positron polarisation the goal of $\delta \sin^2 \theta_{eff} \sim 10^{-5}$ can be reached.

As an example of the potential of the GigaZ $sin^2\theta_{eff}$ measurement Fig. 2 compares the present experimental accuracy on $sin^2\theta_{eff}$ and M_W from LEP/SLD/Tevatron and the prospective accuracy from the LHC and from a LC without GigaZ option with the predictions of the SM and the MSSM. With GigaZ a severe test of the theory will be possible.

3.3 QCD Working Group

Strong–interaction measurements at TESLA will form an important component of the physics programme. The LC offers the possibility of testing QCD at high energy scales in the experimentally clean, theoretically tractable e^+e^- environment. For the LC also the $\gamma\gamma$, γe^- and e^-e^- modes are discussed where one can e.g. study structure functions of photons. Since these modes require a future upgrade we confine ourselves here to only the e^+e^- mode.

The top quark is by far the heaviest fermion observed, yet all the experimental results tell us that it behaves exactly as would be expected for a third generation. Its large mass, which is close to the scale of electroweak symmetry breaking, renders the top quark a unique object for studying the fundamental interactions in the attometer regime. It is likely to play a key role in pinning down the origin of electroweak symmetry breaking. High precision measurements of the properties and the interaction of top quarks will therefore be an essential part of the LC research program.

3.3.1 Polarization effects in production of light quarks

The scaling factors, κ, for the production of the light quarks, $e^+e^- \to q\bar{q}$ with $q = u$, d, c, s, b, are given for $\sqrt{s} = 500$ GeV by [16]:

$$\kappa = \frac{\sigma^{pol}}{\sigma^{unpol}} = [1 - P_{e^-}P_{e^+}][1 - 0.46P_{eff}], \tag{9}$$

where the factor 0.46 is valid for the sum of light quarks. In Table 5 scaling factors for different configurations are listed and one can see that for left–handed electron polarization one gains about 50% in rate if one simultaneously uses right–handed positrons. Conversely, for right–handed electrons the scaling factor increases by about 30% when positron have left–handed polarization.

The main background comes from $e^+e^- \to W^+W^-$. The scaling factors for this reaction are shown in Table 2. The spin configuration (LR) improves the ratio for quark production. However, if right–handed electrons are used, the WW background is strongly suppressed, whereas for the configuration (RL) quark production is suppressed by a factor 0.87. In this case S/B improves by nearly a factor of 3 and $S/\sqrt{B}$ by a factor of 2.

In [17] polarization effects were studied at the top threshold. To determine the top vector couplings, v_t one has to measure the left–right asymmetry A_{LR} with high accuracy. With an integrated luminosity of $\mathcal{L} = 300$ fb^{-1} precisions in A_{LR} and v_t of about 0.4% and 1% respectively can be achieved at the LC. The gain in using simultaneously polarized e^- ($|P_{e^-}| = 80\%$) and e^+ ($|P_{e^+}| = 60\%$) beams is given by the higher effective polarization of $P_{eff} = 0.946$ compared to the case for only polarized electrons. This enhancing of effective polarization is also significant when measuring the decays of polarized top quarks at rest, where the lepton angular distribution of $t \to bW^+(\to e^+\nu)$ is sensitive to the Lorentz structure of the charged currents. The angular distribution of $t \to H^+b$ can be used to directly determine $\tan\beta$. With $\mathcal{L} = 300$ fb^{-1} the coefficients of the angular dependent terms can be determined with accuracies of about 1–2% at a LC.

3.3.2 Polarization effects in limits for top FCN couplings

Recently a study concerning polarization effects of simultaneously polarized e^- and e^+ beams in measuring top flavour changing neutral (FCN) couplings has appeared [18]. In Table 6 the limits on top FCN decay branching ratios obtained from single top production, $e^+e^- \to t\bar{q}$, are listed. The study was made at $\sqrt{s} = 500$ GeV with $\mathcal{L} = 300$ fb^{-1} and $\sqrt{s} = 800$ GeV with $\mathcal{L} = 500$ fb^{-1}. With e^- and e^+ polarization, limits are improved by about a factor 2.5, wheras in each case the positron polarization improves the limits obtained with only electron polarization by 30%–40%, Table 6. Analogoues results can be obtained at $\sqrt{s} = 800$ GeV. These improvements, due to the use of polarized e^+ and e^- beams correspond to an increase of luminosity by a factor of 6–7. Comparison with the limits for FNC couplings from LHC show that the LC measurements are complementary, perhaps even decisive e.g. for the γtu–coupling [18].

The dominant background for the $t\bar{q}$ signal is given by $W^+q\bar{q}'$ production with W^+ decays into lepton pairs. With $|P_{e^-}| = +80\%$ background decreases by a factor of 5 while keeping 90% of the signal. With $|P_{e^-}| = 80\%$ and $|P_{e^+}| = 45\%$ the background is reduced by a factor of 8 and the signal is even increased by 20% compared to the values for unpolarized beams [18].

3.3.3 Polarized structure functions

Up to now nothing is known about polarized structure functions (PPSF) of photons but a LC, especially when operated in the $\gamma\gamma$ or $e^-\gamma$ mode, is well suited to make such studies. For TESLA the $\gamma\gamma$ option has been discussed as a possible upgrade, but it is already possible to get information about PPSF even in the normal e^+e^- mode if one uses highly polarized e^+ and e^- beams.

In [19] studies of PPSF were made in $e^+e^- \to \gamma\gamma + e^+e^- \to$ Di-jets + e^+e^-, using polarized beams. It was found that the structure functions could be extracted from measurements of the asymmetry of the di–jets, $A^{2-\mathrm{jet}}$. Both of the γ's have to be polarized, and because depolarization tends to be large at the $e\gamma$ vertex one needs highly polarized e^- and e^+ beams. In Fig. 3 we show the results of the study when $P_{e^-} = 70\% = P_{e^+}$ and $\sqrt{s} = 500$ GeV. Unfortunately the di–jet asymmetries, $A^{2-\mathrm{jet}}$, are only about 1%, and with a data sample of $\mathcal{L}_{ee} = 10\mathrm{fb}^{-1}$ the errors are 0.5%. With $\mathcal{L}_{ee} = 100\mathrm{fb}^{-1}$, which should be reachable at TESLA the errors would be reduced by a factor of three. Further improvements are possible by optimizing cuts on the data. Thus at least some initial information about PPSF may be obtainable at a LC in the e^+e^- mode, and could establish PPSF for polarized photons. For this purpose it may be necessary to operate with the highest possible positron polarization even at the expense of reduced beam intensity [20].

3.4 Alternative Theories Working Group

Beam polarization is a helpful tool to enlarge the discovery reach of Z', W' and to look for the effects of extra dimensions. Also discrimination between different contact interactions should be simplified with the help of beam polarization.

3.4.1 Polarization effects in discovery reach for Z' and W'

Studies have been made for direct and indirect evidence for production of Z' bosons at a linear collider having $\sqrt{s} = 500$ GeV [21]. Beam polarization enlarges the discovery reach but the predicted effects are strongly model dependent. In Table 7 the lower bound for $m_{Z'}$ at a LC with $\mathcal{L} = 500$ fb^{-1} are presented for two different models, one a superstring–inspired E_6 model and the other a LR model with an additional neutral gauge boson Z'. It can be seen from Table 7 that with $P_{e^-} = 80\%$ and $P_{e^+} = 60\%$ the discovery reach is increased by 10%–20% compared to the case when only $P_{e^-} = 80\%$. The effects of positron polarization in the production of W' bosons are not yet available. In Table 7 we summarize the results of studies made for unpolarized beams, and for polarized electrons with $P_{e^-} = 80\%$ [22] for a LC with $\mathcal{L} = 1$ ab^{-1}. We estimate a roughly 10% increase in the production of left–chirality–prefering W' bosons when $P_{e^-} = 80\%$ and $P_{e^+} = 60\%$ as compared to when only $P_{e^-} = 80\%$, since the effective polarization is increased from 80% to 95%.

In search for right–handed neutral gauge bosons polarization will not only to increase the rate, but even more important it can be used to make major reductions in backgrounds caused by standard left–handed interactions. For example, with $P_{eff} = 95\%$ the left–handed background is reducced by a factor of twenty compared to the case of unpolarized beams.

3.4.2 Polarization effects in contact interactions

Beam polarization is a useful tool to look for the existence of contact interactions and to distinguish between different models. Simulation studies are given in [21] for $\sqrt{s} = 500$ GeV and $\mathcal{L} = 1$ fb^{-1}. In Figure 4 the expected sensitivity from $e^+e^- \to b\bar{b}$ is listed for different models of couplings. Systematical errors are included. One sees that using simultaneous $|P_{e^-}| = 80\%$ and $|P_{e^+} = 40\%|$ instead of only $|P_{e^-} = 80\%|$ could enlarge the discovery reach for the scale Λ by up to 40% for RR or RL interactions.

3.4.3 Polarization effects in discovery reach for extra dimensions

In the search for extra dimensions, $e^+e^- \to \gamma G$, beam polarization enlarges the discovery reach for the scale M_D [23], and is a crucial tool for suppressing the dominant background $e^+e^- \to \nu\bar{\nu}\gamma$ [24]. In Table 8 the lower bounds of M_D are given for various numbers of extra dimensions. The study was made for $\sqrt{s} = 800$ GeV and $\mathcal{L} = 1$ ab^{-1}. With simultaneous beam polarization of $P_{e^-} = 80\%$ and $P_{e^+} = 60\%$ the reach is enlarged by 16% compared to the case with only electron polarization. With increasing numbers of extra dimensions this factor decreases up to 10%. In Figure 5 the cross section for $e^+e^- \to G\gamma$ as a function of M_D is plotted for different systematic errors [23]. For example with unpolarized beams in the case of two extra dimensions, $\delta = 2$, and $M_D = 7.5$ GeV the signal, S, is about three orders of magnitude smaller than the background, B [24]. However, if polarized beams are used the ratio $\frac{S}{\sqrt{B}}$ is improved by 2.2 for $P_{e^-} = 80\%$ and by 5.0 for $P_{e^-} = 80\%$ and $P_{e^+} = 60\%$ as shown in Figure 6. This corresponds to an increase in luminosity by a factor 5 when only electrons are polarized, and a factor 25 when both beams are polarized. In studies for indirect limits on extra dimensions the simultaneous polarization of both beams does not play a significant role. In this case P_{e^+} improves the limits by only 8% [25].

3.5 SUSY Working Group

In SUSY models all coupling structures consistent with Lorentz invariance are possible. Therefore it is possible to get appreciable event rates for polarization configurations that are unfavorable for SM processes. Polarization effects can play a crucial role in discovering SUSY and in the determination of supersymmetric model parameters. All numerical values quoted below, if not otherwise stated, are given for the LC–reference scenario for low $\tan\beta$ with the SUSY parameters $M_2 = 152$ GeV, $\mu = 316$ GeV, $\tan\beta = 3$ and $m_0 = 100$ GeV [26].

3.5.1 Polarization Effects in the Stop Sector

In [27] the feasibility of determining the stop mixing angle in the process $e^+e^- \to \tilde{t}_1\tilde{t}_1$ at the LC has been investigated. The study was made at $\sqrt{s} = 500$ GeV with $\mathcal{L} = 2 \times 500$ fb^{-1}, $|P_{e^-}| = 80\%$ and $|P_{e^+}| = 60\%$ for the parameters $m_{\tilde{t}_1} = 180$ GeV, $\cos\Theta_{\tilde{t}_1} = 0.57$. Measuring the cross sections result in $\delta(m_{\tilde{t}_1}) = 1.1$ GeV and $\delta(\cos\Theta_{\tilde{t}_1}) = 0.01$. If only polarized electrons were used then the error would increase by about 20% [27].

3.5.2 Polarization effects in slepton production

With beam polarization the nature of the SUSY partners of the left– and right–handed particles can easily be identified. The production of sleptons $e^+e- \to \tilde{\ell}_L\tilde{\ell}_L$, $e^+e- \to \tilde{\ell}_R\tilde{\ell}_R$ proceeds via γ and Z exchange in the direct channel and $\tilde{\chi}^0_i$ exchange in the crossed channels. The process $e^+e- \to \tilde{e}_L\tilde{e}_R$ is only possible via the crossed channel. Beam polarization is a valuable tool to separate ℓ_L from ℓ_R [28].

In MSSM scenarios one generally finds that $m_{\tilde{\ell}_R} < m_{\tilde{\ell}_L}$, because only in extended models can this mass hierarchy be weakened [29]. Therefore one can distinguish between the left and right selectron in the pair by measuring the threshold cross sections $(\tilde{e}_R, \tilde{e}_R)$, $(\tilde{e}_R, \tilde{e}_L)$ and $(\tilde{e}_L, \tilde{e}_L)$. The two–body kinematics allows the identification and accurate measurement of the masses, branching ratios, couplings and mixing parameters.

Polarisation is indispensable to determine the weak quantum numbers R, L of the sleptons. Polarization of both beams facilitates the identification of the superpartners of left and right selectrons in a straight–forward manner. S–channel processes are suppressed when both beams are left polarized or both beams are right polarized. In the limit of completely left (or right) polarized beams slepton production can only occur via the t–channel. Measurement of the threshold curves and identification of the sleptons via charge provides a simple and unique method to identify the SUSY partners of left–, right–handed e^- and e^+. Simultaneous polarization of both beams with $|P_{e^-}| = 80\%$ and $|P_{e^+}| = 60\%$ can enhance the signal by a factor 1.8 compared to the case with only electron polarization [30].

In the reaction $e^+e^- \to \tilde{\mu}\tilde{\mu}$, only the pairs $\tilde{\mu}_L\tilde{\mu}_L$, $\tilde{\mu}_R\tilde{\mu}_R$ are produced because the t–channel drops out. The scaling factor and ratio are about the same as in selectron production.

3.5.3 Polarization effects in the chargino sector

As one can see in Fig. 7 beam polarization can considerably enhance the cross section for chargino production. For $|P_{e^-}| = 80\%$ the event rate is enhanced by about a factor 1.8. Simultaneous positron polarisation of $P_{e^+} = 60\%$ leads to an additional increase of a factor 1.6. This increase can not be compensated by higher effective polarization of e^- beams.

In the MSSM the chargino sector depends on the fundamental parameters M_2, μ, $\tan\beta$. Beam polarization is crucial for determining these parameters [31]. The analysis was made for completely longitudinally polarized beams and the assumption that the masses of the exchanged sneutrinos $m_{\tilde{\nu}}$, are known. Using these assumptions it has been shown [31] that these parameters can be determined quite well. Since completely polarized beams do not exist, any efforts to increase the effective polarization are important to improve the accuracy of the results, which means that positron polarization is very advantageous.

In one method to constrain $m_{\tilde{\nu}}$ indirectly [32], beam polartization can be used to help decrease the statistical error, Figur 8. There it is shown that the forward–backward–asymmetry of the decay electron in $e^+e^- \to \tilde{\chi}_1^+\tilde{\chi}_1^-$, $\tilde{\chi}_1^- \to \tilde{\chi}_1^0 e^-\bar{\nu}$, is very sensitive to $m_{\tilde{\nu}}$. With additional positron beam polarization there is a further increases in the cross section by a factor of about 1.6, so that the statistical error in ΔA_{FB} is reduced by at least 20%.

In single chargino production, $e^+e^- \to \tilde{e}\tilde{\chi}^-\nu_e$, $e^+e^- \to \tilde{e}\tilde{\chi}^+\bar{\nu}_e$ [2] the preferred beam polarisation configurations are (RR) and (LL), which are not favored in the SM. The event rates are expected to be small so that positron polarization could play a major role in the analysis and the measurement of this process.

3.5.4 Polarization effects in the neutralino sector

Here, too, beam polarization can significantly enhance the signal and therefore improve the ratios S/B and $S/\sqrt{B}$. As can be seen in Figure 9a the cross section $\sigma(\tilde{\chi}_1^0\tilde{\chi}_2^0)$ can be enhanced by about 60% for $P_{e^-} = -80\%$ and $P_{e^+} = 60\%$ compared to the case of $P_{e^-} = -80\%$ and unpolarized positrons. For right–polarized electrons similar results are obtained e.g. for $\sigma(\tilde{\chi}_2^0\tilde{\chi}_2^0)$, Figure 9b. For this process an even greater advantage of polarizing both beams with different signs is the suppression of the dominant WW background.

Beam polarization may be crucial for the determination of the parameters and the couplings of the neutralino sector of supersymmetric models. In lowest order neutralino production occurs via Z, $\tilde{e}_L$ and $\tilde{e}_R$ exchange, so it is sensitive to the chiral couplings and the masses of $\tilde{e}_L$, $\tilde{e}_R$. The ordering of the cross sections for all different polarization configurations is interesting depending on the character of the neutralinos:

- Pure higgsino:
$$\sigma^{LR} > \sigma^{RL} > \sigma^{L0} > \sigma^{00} > \sigma^{R0} > \sigma^{LL} > \sigma^{RR} \tag{10}$$

- Pure gaugino and $m_{\tilde{e}_L} \gg m_{\tilde{e}_R}$:
$$\sigma^{RL} > \sigma^{R0} > \sigma^{00} > \sigma^{RR} > \sigma^{LL} > \sigma^{L0} > \sigma^{LR} \tag{11}$$

- Pure gaugino and $m_{\tilde{e}_L} \ll m_{\tilde{e}_R}$:
$$\sigma^{LR} > \sigma^{L0} > \sigma^{00} > \sigma^{LL} > \sigma^{RR} > \sigma^{R0} > \sigma^{RL} \tag{12}$$

If only the electron is polarized then the orderings of the cross sections for the cases (10) and (12) are equal. If, however, both beams are simultaneously polarized the three cases could be distinguished [32].

If the selectrons are too heavy to be produced in the direct channel one may still be able to constrain the selectron masses by studying forward–backward asymmetries, A_{FB}, in the production and decay of neutralinos [32]. Neutralinos are Majorana particles, so that if CP is conserved, then neutralino production is exactly forward–backward symmetric. However, due to spin correlations between production and decay, $A_{FB} \neq 0$ for the decay electron can occur, e.g. in the reactions $e^+e^- \to \tilde{\chi}_1^0\tilde{\chi}_2^0$, $\tilde{\chi}_2^0 \to \tilde{\chi}_1^0 e^+e^-$ [33]. Beam polarization enlarges these asymmetries by about a factor 3 if both beams are simultaneously polarized (Figure 10a). In this case the magnitude of A_{FB} can be as large as 13%, wheras in the case of unpolarized positrons, only 4% is possible. Moreover, for a given electron polarization even the sign of A_{FB} can change when using polarized positrons. The A_{FB} of the neutralino decay products are sensitive to the selectron masses $m_{\tilde{e}_L}$, $m_{\tilde{e}_R}$ as can be seen in Figure 10b. If direct production of selectron pairs is kinematically not accessible, studying A_{FB} allows constraining the selectron masses. Since in the configuration (LR) both the cross sections and the asymmetries are larger than those for (L0) the simultaneous polarization of both beams increases the accuracy of indirectly determined masses of the particles.

Beam polarization is also helpful for constraining the M_1 parameter of the MSSM [32]. As can be seen in Figures 11a, b the cross section, e.g. $\sigma(e^+e^- \to \tilde{\chi}^0_1\tilde{\chi}^0_2) \times BR(\tilde{\chi}^0_2 \to \tilde{\chi}^0_1 e^+e^-)$, as well as the A_{FB} of the decay electron are very sensitive to the M_1 parameter. In regions of the parameter space where it is possible to determine M_1 by measuring the neutralino masses [34] this method would provide an independent check. Figure 11a shows that when both beams are polarized the cross sections increase by a factor of about 1.6 and the statistical error is reduced by a factor of about 0.8 compared to the case when only the electron beam is polarized. This reduction would improve the accuracy of A_{FB} by about 20%, Figure 11b.

The MSSM contains 4 neutralinos. One additional Higgs singlet yields the (M+1)SSM, with 5 neutralinos. Superstring–inspired E_6–models with even more neutral gauge bosons or Higgs singlets have a spectrum of 6 or more neutralinos. In certain regions of the parameter space, where the lightest neutralino is singlino–like, the same mass spectra of the light neutralinos are possible in the MSSM, NMSSM and E_6. Beam polarization is sensitive to the different couplings, and can be used to distinguish between possible models [35, 36]. For example, Figure 12a shows that the models can be separated by comparing the cross sections. If only the electron is polarized the difference between the MSSM cross section of about 6 fb and the (M+1)SSM cross section of 7.5 fb is rather small. For $P_{e^-} = 80\%$ and $P_{e^+} = 60\%$ this difference would be larger by more than a factor 2. In this case the cross sections are about 7 fb in the MSSM and up to about 10.5 fb in the (M+1)SSM, so that it would become easier to distinguish the models.

In the E_6 model the cross sections show the same dependence on beam polarization [35] but they are much smaller due to the large singlino component in the LSP. One gets less than 1.5 fb in the unpolarized case and less than about 3 fb if only the electron beam is polarized. However, with $P_{e^-} = 80\%$ and $P_{e^+} = 60\%$ one can reach 5 fb, which could be decisive for measuring the process (Figure 12b). This example also shows that polarizing the e^+ beams not only increases the effective polarization but can be used to significantly enhance the event rates.

3.5.5 Polarization effects in R–parity violating SUSY

In R–parity violating SUSY, processes can occur which prefer the extraordinary (LL) or (RR) polarization configurations. An interesting example is $e^+e^- \to \tilde{\nu} \to e^+e^-$. The main background to this process is Bhabha scattering. Polarizing both electrons and positrons can greatly suppress this background, while at the same time it enhances the signal. A study [37] was made for $m_{\tilde{\nu}} = 650$ GeV, $\Gamma_{\tilde{\nu}} = 1$ GeV, with an angle cut of $45^0 \leq \Theta \leq 135^0$ and a lepton–number violating coupling $\lambda_{131} = 0.05$ in the R–parity violating Langrangian $\mathcal{L}_{\not{R}} \sim \sum_{i,j,k} \lambda_{ijk} L_i L_j E_k$. Here $L_{i,j}$ denotes the left–handed lepton and squark superfield and E_k the corresponding right–handed field [37].

The resonance curve for the process, including the complete SM–background is given in Figure 13. The event rates at the peak are given in Table 9. Electron polarization alone with $P_{e^-} = -80\%$ enhances the signal only by 7%, whereas the simultaneous polarization of both beams with $P_{e^-} = -80\%$ and $P_{e^+} = -60\%$ produces a further increase by about 25%.

This configuration of beam polarizations, which strongly suppresses pure SM processes, allows one to perform a fast diagnostics for this R–parity violating process. For example the process $e^+e^- \to Z'$ could lead to a similar resonance peak, but with different polarization dependence. Here only the 'normal' configurations LR and RL play a role and this process will be strongly suppressed by LL. Therefore such a resonance curve, Figure 13, with different beam polarizations would uniquely identify an an R–parity violating SUSY process.

4 Summary

The clean and fundamental nature of e^+e^- collisions in a linear collider is ideally suited for the search for new physics, and the determination of both Standard Model and New Physics couplings with high precision. Polarization effects will play a crucial role in these processes. The fact that highly polarized electron beams are easily achievable in a linear collider has already been demonstrated at the SLAC SLC, and there is every reason to expect that electron polarizations in excess of 80% will be possible at future linear colliders. Methods for achieving 40–60% positron polarization have been developed, and in this paper we have shown that simultaneous polarization of both beams can significantly expand the accessible physics opportunities. Our main conclusions are summarized in Table 1, where we list the quantitative improvements when simultaneously polarized e^- and e^+ beams are used compared to the case where only polarized electrons but unpolarized positrons are used.

A recurring theme in this paper is that the simultaneous polarization of both electrons and positrons can be used to determine quantum numbers of new particles, increase rates, decrease background, raise the effective polarization, reduce the error in determining the effective polarization, distinguish between competing interaction mechanism, and expand the range of measurable experimental observables. These virtues help to provide us with unique new insights into Higgs, Electroweak, QCD, SUSY processes and Alternative Theories.

We have shown that polarization is an essential ingredient in the determination of Higgs couplings. In the electroweak sector, the use of polarized beams should make possible an order–of–magnitude reduction in the error of the weak mixing angle over the present value. Such a measurement would give us unprecedented sensitivity to radiative corrections caused by processes at otherwise unattainable energy scales (GigaZ). In QCD polarization influences quark production and improves considerably the accuracy in determining e.g. the top couplings. With highly polarized e^+ and e^- it should be possible to establish polarized photon structure functions. In the search for new gauge bosons, contact interactions and extra dimension polarization is crucial to enhance rates and suppress background. Finally, in the yet undiscovered world of SUSY interactions critical polarization effects abound e.g. for the discovery and especially in the determination of the basic coupling parameters. Non–standard polarization configurations can be used to determine fundamental quantum numbers of SUSY particles. For all of these reasons, and perhaps some that we havn't thought of yet, polarized electron and positron beams should be an integral part of future linear colliders.

We would like to thank M. Battaglia, T. Behnke, A. Brandenburg, A. De Roeck, K. Desch, M. Diehl, H. Eberl, K. Flöttmann, H. Fraas, F. Franke, N. Ghodbane, S. Hesselbach, R. Heuer, J. Kalinowski, W. Kilian, B. Kniehl, S. Kraml, J. Kühn, W. Majerotto, U. Martyn, W. Menges, K. Mönig, T. Ohl, S. Riemann, P. Schüler, R. Settles, H. Spiesberger, M. Stratmann, A. Vogt, N. Walker, G. Weiglein, G. Wilson, P. Zerwas for interesting discussions.

References

[1] SLAC–Report 485, submitted to Snowmass 96.

[2] Ch. Baltay, ECFA/DESY LC–workshop, Obernai, October 1999.

[3] V.E. Balakin and A.A. Mikhailichenko, INP 79–85 (1979).

[4] K. Flöttmann, DESY-93-161, 1993; N. Walker, ECFA/DESY LC–workshop, Hamburg, September 2000.

[5] DESY Reports 92-123 A+B, 93-123 C, 96-123 D, 99-123F, P.M. Zerwas *ed.*.

[6] K. Desch, ECFA/DESY LC–workshop, Obernai, October 1999.

[7] A. Gurtu, talk given at ICHEP 2000, Osaka, July 2000, to appear in the proceedings.

[8] S. Heinemeyer, W. Hollik, G. Weiglein, EPJ C 9 (1999) 343.

[9] B. Kniehl, ECFA/DESY LC–workshop, Hamburg, September 2000.

[10] D. Atwood, A. Soni, Phys. Rev. D45 (1992)2405; M. Davier, L. Duflot, F. Le Diberder, A. Rouge, Phys. Lett. B306 (1993) 411; M. Diehl, O. Nachtmann, Z. Phys. C62 (1994) 397; K. Hagiwara, S. Ishihara, J. Karnoshita, B.A. Kniehl, Eur. Phys. J. C14 (2000) 457.

[11] R. Hawkings and K. Moenig, EPJ*direct* C 8 (1999) 1.

[12] W. Menges, *A Study of Charged Current Triple Gauge Couplings at TESLA*, LC–PHSM–2001–022.

[13] S. Heinemeyer, Th. Mannel, G. Weiglein, hep-ph/9909538, LC Workshop, Sitges 1999; J. Erler, S. Heinemeyer, W. Hollik, G. Weiglein, P.M. Zerwas, Phys. Lett. **B486** (2000) 125; S. Heinemeyer, G. Weiglein, hep-ph/0012364, LCWS 2000, Chicago, Ocober 2000.

[14] A. Blondel, Phys. Lett. **B202** (1988) 145.

[15] K. Hagiwara, R.D. Peccei, D. Zeppenfeld, K. Hisaka, Nucl. Phys. **B282** (1987) 253.

[16] A. Brandenburg, ECFA/DESY LC–workshop, Obernai, October 1999; private discussion with A. Brandenburg.

[17] J.H. Kühn, *Polarized Beams and the top threshold*, LC–TH–2001-04.

[18] J.A. Aguilar-Saavedra, hep-ph/0012305.

[19] M. Stratmann, Nucl. Phys. Proc. Suppl. 82 (2000) 400; private discussion with M. Stratmann and A. Vogt.

[20] Private discussion with A. de Roeck.

[21] A. Leike, S. Riemann, Z. Phys.C75 (1997) 341; S. Riemann, hep-ph/9610513, Proceedings of the 1996 DPF / DPB Summer Study on New Directions for High-energy Physics; R. Casalbuoni, S. De Curtis, D. Dominici, R. Gatto, S. Riemann, hep-ph/0001215, LC-TH-2000-006; S. Riemann, Proceedings of 4th International Workshop on Linear Colliders (LCWS 99), Sitges, Barcelona, Spain; S. Riemann, LC-TH-2001-007.

[22] S. Godfrey, P. Kalyniak, B. Kamal, A. Leike, Phys. Rev. D61 (2000) 113009.

[23] A. Vest,*Search for extra dimensions in graviton emission* $e^+e^- \to \gamma G$, LC–TH–2000–058.

[24] G. Wilson, ECFA/DESY LC–workshop, Padua, May 2000.

[25] S. Riemann, to appear in the Proceedings of the 5th International Linear Collider Workshop (LCWS2000), Fermilab, Batavia, Illinois, Oct.24-28, 2000.

[26] S. Ambrosanio, G.A. Blair, P.M. Zerwas, EFCA/DESY LC–workshop, 1998.

[27] A. Bartl, H. Eberl, S. Kraml, W. Majerotto, W. Porod, EPJdirect C6 (2000) 1, LC–TH–2000–031; private discussion with S. Kraml.

[28] M. Dima, LCWS 2000, Chicago, October 2000.

[29] S.P. Martin, P. Ramond, Phys. Rev. D48 (1993) 5365.

[30] N. Ghodbane, calculated with Susygen, private discussion.

[31] S.Y. Choi, A. Djouadi, M. Gouchait, J. Kalinowski, H.S. Song, P.M. Zerwas, Eur. Phys. J. C14 (2000) 535, LC–TH–2000-016.

[32] G. Moortgat–Pick, A. Bartl, H. Fraas, W. Majerotto, Eur. Phys. J. C18 (2000) 379; G. Moortgat–Pick, A. Bartl, H. Fraas, W. Majerotto, LC–TH–2000–032, hep-ph/0002253; G. Moortgat–Pick, A. Bartl, H. Fraas, W. Majerotto, LC–TH–2000-033, hep-ph/0004181; G. Moortgat-Pick, H. Fraas, Acta Phys. Polon. B30 (1999) 1999 .

[33] G. Moortgat–Pick, H. Fraas, Phys. Rev. D59 (1999), 015016; G. Moortgat–Pick, H. Fraas, A. Bartl, W. Majerotto, Eur. Phys. J. C9 (1999) 521, Eur. Phys. J. C9 (1999) 549 (E); G. Moortgat-Pick, H. Fraas, hep-ph/0012229.

[34] J.L. Kneur, G. Moultaka, Phys. Rev. D59 (1999) 015005.

[35] G. Moortgat–Pick, F. Franke, S. Hesselbach, H. Fraas, Proceedings of the LC–Workshop, Sitges 1999; S. Hesselbach, F. Franke, H. Fraas, LC–TH–2000–025, hep-ph/0003272.

[36] F. Franke, S. Hesselbach, private discussion.

[37] M. Heyssler, R. Rückl, H. Spiesberger, Proceedings of the LC–Workshop, Sitges 1999; private discussion with H. Spiesberger.

Process	Background	Further Improvements by $P(e^+)$	
Higgs			
$e^+e^- \to H\bar{\nu}\nu$	WW, ZZ, $Z\bar{\nu}\nu$	Enhancing of $\frac{S}{B}$, $\frac{S}{\sqrt{B}}$	20%–30%
$e^+e^- \to HZ$		better separation: $HZ \leftrightarrow H\bar{\nu}\nu$	factor 4
	$W^{\pm}\ell^{\mp}\overset{(-)}{\nu}$	suppression of single W	important
$e^+e^- \to HZ \to H\bar{f}f$		general HZV	error reduction by 30%
Electroweak			
high $\sqrt{s}$:			
$e^+e^- \to W^+W^-$	$\gamma\gamma \to W^+W^-$	Enhancing of $\frac{S}{B}$, $\frac{S}{\sqrt{B}}$	
	$W^{\pm}Z\nu$, W^+W^-Z	$\Delta\kappa_\gamma$, $\Delta\lambda_\gamma$, $\Delta\kappa_Z$, $\Delta\lambda_Z$,	error reduction by factor 1.8
Giga Z:			
$e^+e^- \to Z$		improve $\delta(P)$, A_{LR}	factor 10
QCD			
$e^+e^- \to q\bar{q}$	$e^+e^- \to W^+W^-$	Enhancing of $\frac{S}{B}$, $\frac{S}{\sqrt{B}}$	factor 2–3
$e^+e^- \to \gamma\gamma \to jets$		pol. structure functions	at least factor 3
$e^+e^- \to t\bar{q}$	$e^+e^- \to Wq\bar{q}'$	Enhancing of $\frac{S}{B}$, $\frac{S}{\sqrt{B}}$	further increase by a factor 2
		Vtq couplings (FCNC)	limits reduction by 40%
SUSY			
$e^+e^- \to \tilde{\ell}\tilde{\ell}$, $\tilde{\chi}^+\tilde{\chi}^-$, $\tilde{\chi}^0\tilde{\chi}^0$	W^+W^-, ZZ	better separation $\tilde{\ell}_L \leftrightarrow \tilde{\ell}_R$	factor 2.5
		Test of quantum numbers L, R	uniquely with LL, RR
		better indirect $m_{\tilde{\nu}}$	
		separation between models	important
		Enhancing of $\frac{S}{B}$, $\frac{S}{\sqrt{B}}$	factor 2–3
		error reduction in M, μ, $\tan\beta$	
$e^+e^- \to \tilde{\chi}^{\pm}\tilde{e}\nu$		enhancement with LL, RR	probably essential
Alternative Theories			
$e^+e^- \to \gamma, Z, Z', W'W'$	W^+W^-, $W^{\pm}e^{\mp}\nu$, WWZ, $f\bar{f}$, ZH	Enhancing of $\frac{S}{B}$, $\frac{S}{\sqrt{B}}$	model dependent
		discovery reach of W', Z'	enlarged by about 10% − −20%
$\not{R}$: $e^+e^- \to \tilde{\nu}_\tau \to e^+e^-$	e^+e^-	Enhancing S/B, $s/\sqrt{B}$	factor 25% with LL
		Test of quantum number	
CI: $e^+e^- \to \mu^+\mu^-$, $q\bar{q}$		sensitivity	enlarged by 40%, O(10^2 TeV)
ED: $e^+e^- \to \gamma G$	$e^+e^- \to \nu\bar{\nu}\gamma$	Enhancing of $\frac{S}{B}$, $\frac{S}{\sqrt{B}}$	up to factor 5
		discovery reach	enlarged by 20%, O(TeV)

Table 1: Summary – polarization effects in all working groups. The improvement factors indicate the gain if one polarizes simultaneously e^- and e^+ beams compared to the case when only e^- is polarized.

Configuration $(sgn(P_{e^-})sgn(P_{e^+}))$	Higgs Production $e^+e^- \to H\nu\bar{\nu}$	$e^+e^- \to HZ$	Background $e^+e^- \to WW$, $e^+e^- \to Z\nu\bar{\nu}$	$e^+e^- \to ZZ$
$(+0)$	0.20	0.87	0.20	0.76
(-0)	1.80	1.13	1.80	1.25
$(+-)$	0.08	1.26	0.10	1.05
$(-+)$	2.88	1.70	2.85	1.91

Table 2: Higgs production in Standard Model: Scaling factors, i.e. ratios of polarized and unpolarized cross section $\sigma^{pol}/\sigma^{unpol}$, are given in Higgs production and background processes for different polarization configurations with $|P_{e^-}| = 80\%$, $|P_{e^+}| = 60\%$ [6].

	$\epsilon_\tau = 0 = \epsilon_b$			$\epsilon_\tau = 50\%$, $\epsilon_b = 60\%$
	$P_{e^-} = 0 = P_{e^+}$	$P_{e^-} = 80\%$, $P_{e^+} = 0$	$P_{e^-} = 80\%$, $P_{e^+} = 60\%$	$P_{e^-} = 80\%$, $P_{e^+} = 60\%$
$\mathrm{Re}(b_Z)$	0.00055	0.00028	0.00023	0.00022
$\mathrm{Re}(c_Z)$	0.00065	0.00014	0.00011	0.00011
$\mathrm{Re}(b_\gamma)$	0.01232	0.00052	0.00036	0.00034
$\mathrm{Re}(c_\gamma)$	0.00542	0.00011	0.00008	0.00007
$\mathrm{Re}(\tilde{b}_Z)$	0.00104	0.00095	0.00078	0.00052
$\mathrm{Re}(\tilde{b}_\gamma)$	0.00618	0.00145	0.00101	0.00063
$\mathrm{Im}(b_Z - c_Z)$	0.01055	0.00070	0.00049	0.00046
$\mathrm{Im}(b_\gamma - c_\gamma)$	0.00206	0.00070	0.00057	0.00054
$\mathrm{Im}(\tilde{b}_Z)$	0.00521	0.00032	0.00022	0.00022
$\mathrm{Im}(\tilde{b}_\gamma)$	0.00101	0.00032	0.00026	0.00026

Table 3: Higgs production – Determination of general Higgs couplings: Optimal errors on general $ZZ\Phi$ and $Z\gamma\Phi$ couplings for different efficiencies ϵ_τ, ϵ_b and beam polarizations [9].

	Δg_1^{Z1}	$\Delta\kappa_\gamma{}^1$	$\lambda_\gamma{}^1$	Δg_1^Z	$\Delta\kappa_\gamma$	λ_γ	$\Delta\kappa_Z$	λ_Z	g_4^Z	g_5^Z	$\tilde{\kappa}_Z$	$\tilde{\lambda}_Z$
unpolarized beams												
$\sqrt{s} = 500$ GeV	7.3	5.7	6.1	38.1	4.8	12.1	8.7	11.5	85.8	27.7	64.9	11.4
$\sqrt{s} = 800$ GeV	4.5	3.1	2.8	39.0	2.6	5.2	4.9	5.1	41.8	28.5	29.6	4.9
only electron beam polarized, $\lvert P_{e^-}\rvert = 80\%$												
$\sqrt{s} = 500$ GeV	4.3	4.2	5.1	24.8	4.1	8.2	5.0	8.9	79.9	22.8	50.6	10.3
$\sqrt{s} = 800$ GeV	2.7	2.3	3.1	21.9	2.2	5.0	2.9	4.7	31.8	24.3	24.1	4.4
both beams polarized, $\lvert P_{e^-}\rvert = 80\%$ and $\lvert P_{e^+}\rvert = 60\%$												
$\sqrt{s} = 500$ GeV	2.8	3.1	4.3	15.5	3.3	5.9	3.2	6.7	45.9	16.5	39.0	7.5
$\sqrt{s} = 800$ GeV	1.8	1.9	2.6	12.6	1.9	3.3	1.9	3.0	18.3	14.4	14.3	3.0

Table 4: Electroweak Theory – Determination of couplings: Expected sensitivity ($\times 10^{-4}$) for different triple gauge couplings κ_V and anomalous triple gauge couplings λ_V in $e^+e^- \to W^+W^-$ at a center-of-mass energy of $\sqrt{s} = 500$ GeV and $\sqrt{s} = 800$ GeV. In the case of polarized beams the luminosity is split up equally on both combinations; δg_1^{Z1}, $\Delta\kappa_\gamma^1$, λ_γ^1 were evaluated by using $SU(2) \times U(1)$ relations [12].

	Configuration of $(sign(P_{e^-})sign(P_{e^+}))$			
scaling factors	$L0$	LR	$R0$	RL
$e^+e^- \to q\bar{q}$	1.37	2.12	0.63	0.87

Table 5: QCD – Quark production: Scaling factors, i.e. ratios of polarized and unpolarized cross sections $\sigma^{pol}/\sigma^{unpol}$, of light quark production $e^+e^- \to q\bar{q}$ at $\sqrt{s} = 500$ GeV [16].

	unpolarized beams	$\|P_{e^-}\| = 80\%$	$\|P_{e^-}\| = 80\%$, $\|P_{e^+}\| = 45\%$
	$\sqrt{s} = 500$ GeV		
$BR(t \to Zq)(\gamma_\mu)$	4.4×10^{-4}	3.1×10^{-4}	1.9×10^{-4}
$BR(t \to Zq)(\sigma_{\mu\nu})$	3.5×10^{-5}	2.4×10^{-5}	1.5×10^{-5}
$BR(t \to \gamma q)$	2.2×10^{-5}	1.3×10^{-5}	8.2×10^{-6}
	$\sqrt{s} = 800$ GeV		
$BR(t \to Zq)(\gamma_\mu)$	4.4×10^{-4}	2.9×10^{-4}	2.4×10^{-4}
$BR(t \to Zq)(\sigma_{\mu\nu})$	1.3×10^{-5}	8.6×10^{-6}	6.2×10^{-6}
$BR(t \to \gamma q)$	7.8×10^{-6}	4.5×10^{-6}	3.7×10^{-6}

Table 6: QCD – Determination of top couplings: Limits 95% C.L. of top flavour changing neutral couplings from top branching fractions at $\sqrt{s} =$ 500 GeV with $\mathcal{L} = 300$ fb^{-1} and at $\sqrt{s} = 800$ GeV with $\mathcal{L} = 500$ fb^{-1} [18].

	$\mathcal{L} = 500$ fb^{-1}		$\mathcal{L} = 1$ ab^{-1}		
	$M_{Z'}$ in E$_6$	$M_{Z'}$ in LR	$M_{W'}$ in SSM	$M_{W'}$ in LR	$M_{W'}$ in KK
unpolarized case	–	–	1.7 TeV	0.9 TeV	1.8 TeV
$\|P_{e^-}\| = 80\%$	4.4 TeV	4.0 TeV	2.2 TeV	1.2 TeV	2.3 TeV
$\|P_{e^-}\| = 80\%$, $\|P_{e^+}\| = 60\%$	4.9 TeV	6.0 TeV	rough approximation: further gain about 20%		

Table 7: Alternative Theories – Reach for additional gauge bosons Z' and W' in different models: Lower bounds of $M_{Z'}$ in an E$_6$– and a LR–model for $\mathcal{L} = 500$ fb^{-1} [21]. Lower bounds of $M_{W'}$ in a model with SM–coupling W', in a LR–model and in a Kaluza–Klein model [22].

Number of Extra Dimensions	Polarisation	M_D/TeV for C.L.= 95 % and $\frac{\Delta f_N}{f_N} = 1\,\%$	Scale M_D/TeV for C.L.= 95 % and $\frac{\Delta f_N}{f_N} = 0.1\,\%$
$\delta = 2$	$P_{e_R^-} = 0$, $P_{e_L^+} = 0$	6.0	6.5
	$P_{e_R^-} = 0.8$, $P_{e_L^+} = 0$	7.4	8.7
	$P_{e_R^-} = 0.8$, $P_{e_L^+} = -0.45$	8.7	10.0
	$P_{e_R^-} = 0.8$, $P_{e_L^+} = -0.6$	9.4	10.8
$\delta = 3$	$P_{e_R^-} = 0$, $P_{e_L^+} = 0$	4.4	4.8
	$P_{e_R^-} = 0.8$, $P_{e_L^+} = 0$	5.2	6.0
	$P_{e_R^-} = 0.8$, $P_{e_L^+} = -0.45$	6.0	6.8
	$P_{e_R^-} = 0.8$, $P_{e_L^+} = -0.6$	6.4	7.3
$\delta = 4$	$P_{e_R^-} = 0$, $P_{e_L^+} = 0$	3.6	3.7
	$P_{e_R^-} = 0.8$, $P_{e_L^+} = 0$	4.2	4.6
	$P_{e_R^-} = 0.8$, $P_{e_L^+} = -0.45$	4.6	5.0
	$P_{e_R^-} = 0.8$, $P_{e_L^+} = -0.6$	4.8	5.3
$\delta = 5$	$P_{e_R^-} = 0$, $P_{e_L^+} = 0$	2.9	3.1
	$P_{e_R^-} = 0.8$, $P_{e_L^+} = 0$	3.3	3.6
	$P_{e_R^-} = 0.8$, $P_{e_L^+} = -0.45$	3.6	3.9
	$P_{e_R^-} = 0.8$, $P_{e_L^+} = -0.6$	3.8	4.2
$\delta = 6$	$P_{e_R^-} = 0$, $P_{e_L^+} = 0$	2.5	2.6
	$P_{e_R^-} = 0.8$, $P_{e_L^+} = 0$	2.8	3.1
	$P_{e_R^-} = 0.8$, $P_{e_L^+} = -0.45$	3.1	3.3
	$P_{e_R^-} = 0.8$, $P_{e_L^+} = -0.6$	3.2	3.4
$\delta = 7$	$P_{e_R^-} = 0$, $P_{e_L^+} = 0$	1.9	2.0
	$P_{e_R^-} = 0.8$, $P_{e_L^+} = 0$	2.2	2.3
	$P_{e_R^-} = 0.8$, $P_{e_L^+} = -0.45$	2.3	2.4
	$P_{e_R^-} = 0.8$, $P_{e_L^+} = -0.6$	2.4	2.6

Table 8: Alternative Theories – Search for extra dimensions in graviton emission: Scale M_D/TeV in dependence of the numbers δ of extra dimensions and different configurations of beam polarizations for $\sqrt{s} = 800\,\mathrm{GeV}$ and $\mathcal{L}_{int} = 1000\,\mathrm{fb}^{-1}$ at a confidence level of 95 % ($\Delta\chi^2 = 3.84$) for the normalisation uncertainties $\frac{\Delta f_N}{f_N} = 1\,\%$ and for $\frac{\Delta f_N}{f_N} = 0.1\,\%$ [23].

	$\sigma(e^+e^- \to e^+e^-)$ with $\sigma(e^+e^- \to \tilde{\nu} \to e^+e^-)$	Bhabha–background
unpolarized	6.99 pb	4.49 pb
$P_{e^-} = -80\%$	7.32 pb	4.63 pb
$P_{e^-} = -80\%$, $P_{e^+} = -60\%$	9.20 pb	4.92 pb

Table 9: SUSY – Sneutrino production in R–parity violating SUSY: Cross sections of $e^+e^- \to \tilde{\nu} \to e^+e^-$ for unpolarized beams, $P_{e^-} = -80\%$ and unpolarized positrons and $P_{e^-} = -80\%$, $P_{e^+} = -60\%$. The study was made for $m_{\tilde{\nu}} = 650$ GeV, $\Gamma_{\tilde{\nu}} = 1$ GeV, an angle cut of $45^0 \le \theta \le 135^0$ and the R–parity violating coupling $\lambda_{131} = 0.05$ [37].

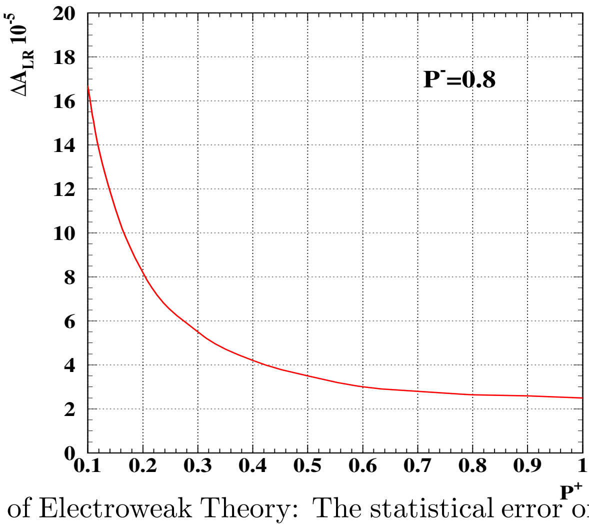

Figure 1: Test of Electroweak Theory: The statistical error on the left–right asymmetry A_{LR} of $e^+e^- \to Z \to \ell\bar{\ell}$ at GigaZ as a function of the positron polarization $P(e^+)$ for fixed electron polarization $P_{e^-} = \pm 80\%$ [11].

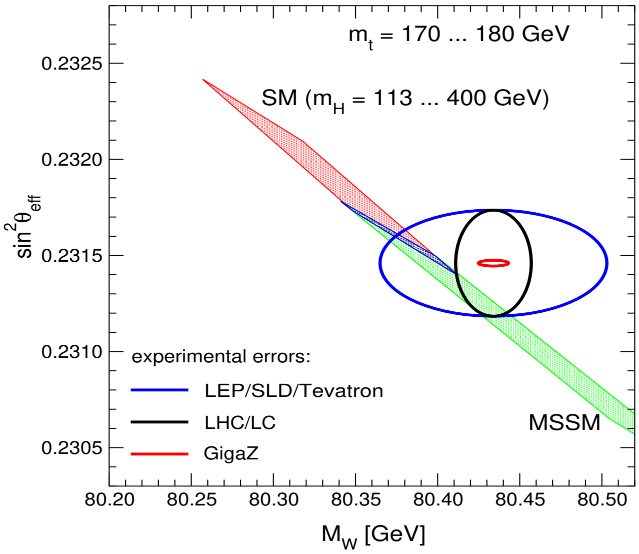

Figure 2: Test of Electroweak Theory: A high-precision measurement at GigaZ of the left–right asymmetry A_{LR} and consequently of $\sin^2\Theta^l_{eff}$ allows to test the electroweak theory at an unprecedented level. The allowed parameter space of the SM and the MSSM in the $\sin^2\Theta^l_{eff}$–M_W plane is shown together with the experimental accuracy reachable at GigaZ. For comparison, the present experimental accuracy (LEP/SLD/Tevatron) and the prospective accuracy at the LHC and a LC without GigaZ option (LHC/LC) are also shown [13].

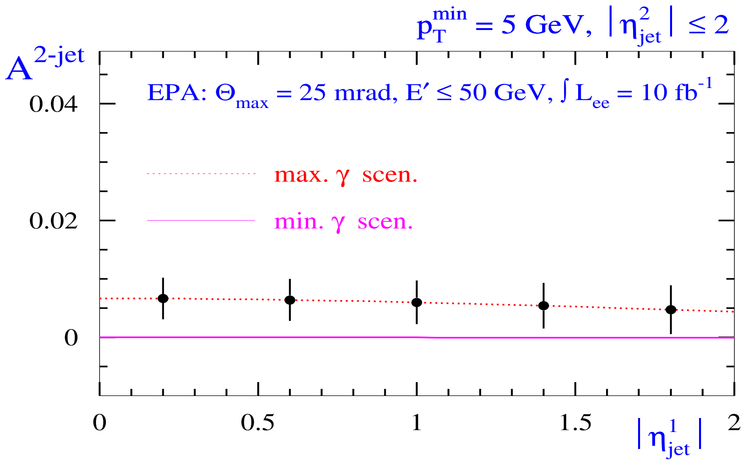

Figure 3: QCD – Establishing of polarized photon structure functions: Di–jet asymmetry of $e^+e^- \rightarrow e^+e^-$+Di–jets for events with $p_T^{jet} = 5$ GeV and $|\eta_{jet}| < 2$ for $\gamma\gamma$ collisions at an e^+e^- collider. Since only $\mathcal{L}_{ee} = 10$ fb^{-1} the statistical errors of the small di–jet asymmetries are quite large, $\sim 0.5\%$. If, however, $\mathcal{L}_{ee} = 100$ fb^{-1} is assumed, which would be reachable at TESLA, the errors are reduced by about a factor 3. Optimization of cuts will further reduce the errors [19].

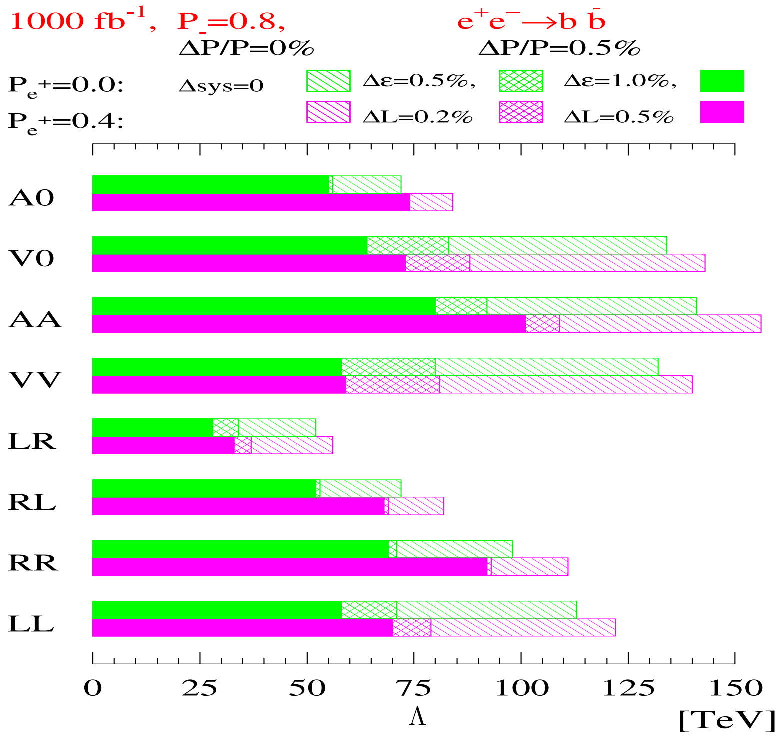

Figure 4: Alternative Theories – Reach for different contact interactions: Expected sensitivities (95%) to contact interaction scales Λ in $e^+e^- \rightarrow b\bar{b}$ at $\sqrt{s} = 500$ GeV with $\mathcal{L} = 1000$ fb^{-1} for $P_{e^-} = 80\%$ and unpolarized positrons and both beams polarized with $|P_{e^-}| = 80\%$, $|P_{e^+}| = 40\%$. [21].

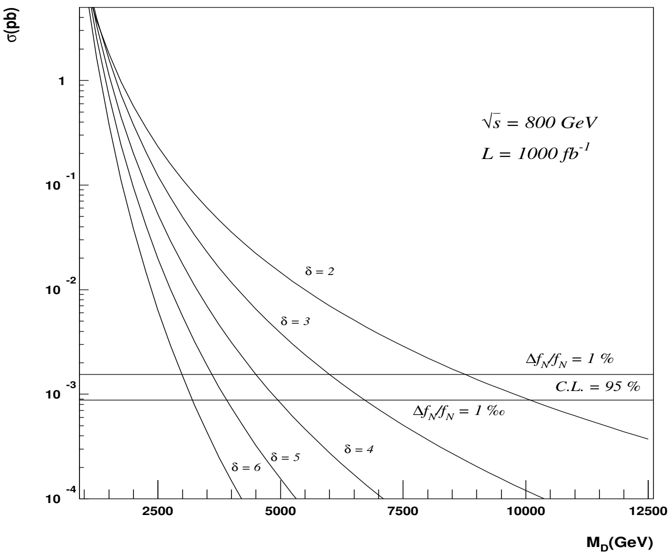

Figure 5: Alternative Theories – Search for extra dimensions in graviton emission: Total cross sections for $e^+e^- \to \gamma G$ with $P_{e^-} = 80\%$ and $P_{e^+} = 60\%$ at $\sqrt{s} = 800$ GeV, $\mathcal{L} = 1000\ \mathrm{fb}^{-1}$ as a function of the scale M_D [TeV] for different numbers δ of extra dimensions. The two horizontal lines indicate two different normalization uncertainties $\frac{\Delta f_N}{f_N} = 1\%$ and $\frac{\Delta f_N}{f_N} = 0.1\%$ [23].

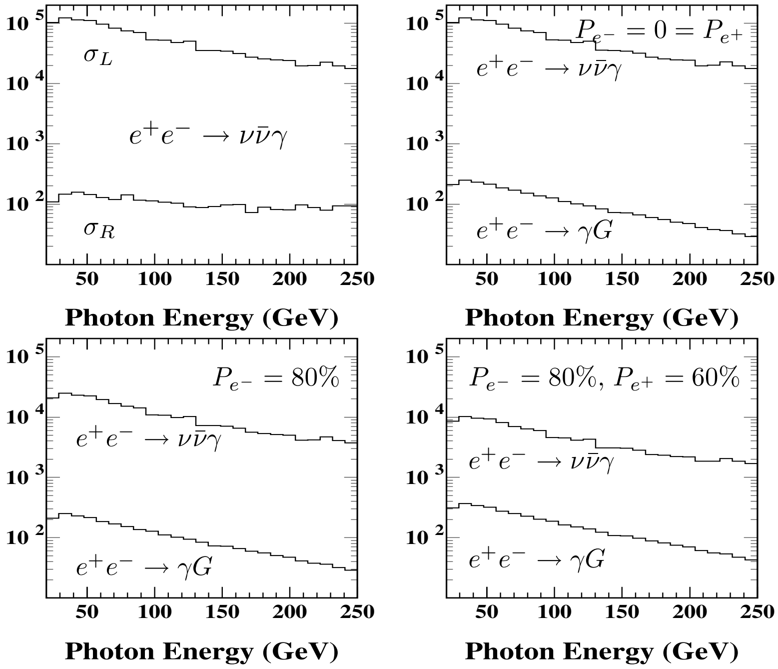

Figure 6: Alternative Theories – Search for extra dimensions in graviton emission: Background $e^+e^- \to \nu\bar{\nu}\gamma$ to direct search $e^+e^- \to \gamma G$ at $\sqrt{s} =$ 800 GeV, $\mathcal{L} = 1000$ fb^{-1} for $\delta = 2$, $M_D = 7.5$ TeV as function of the photon energy for different configurations of beam polarizations. With both beams polarized, $P_{e^-} = 80\%$ and $P_{e^+} = -60\%$ the significance $S/\sqrt{B}$ is improved by a factor 5, with electron polarization but unpolarized positron one gains only the factor 2.2 [24].

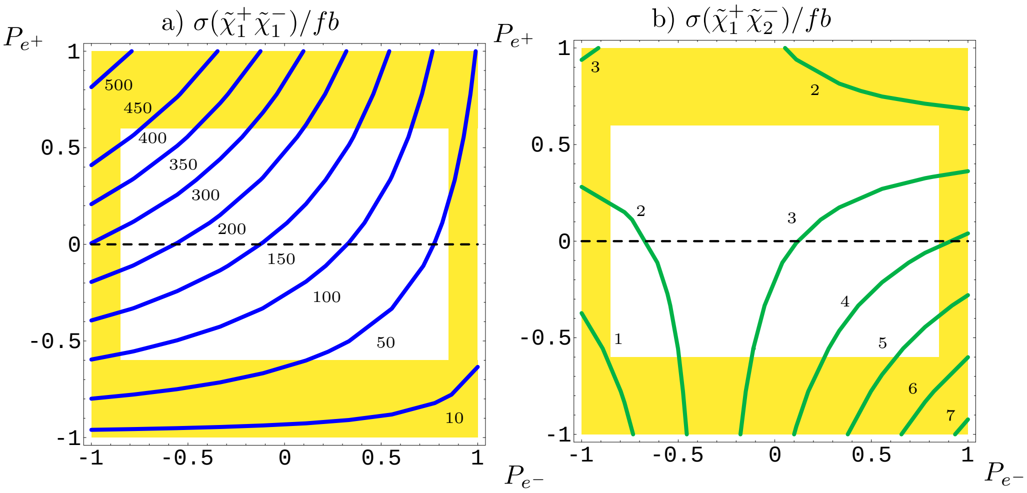

Figure 7: SUSY – Chargino production: Cross sections of $e^+e^- \to \tilde{\chi}_1^+\tilde{\chi}_1^-$, $e^+e^- \to \tilde{\chi}_1^+\tilde{\chi}_1^-$ in fb at $\sqrt{s} = m_{\tilde{\chi}_i^+} + m_{\tilde{\chi}_j^-} + 10$ GeV in the reference scenario for different electron (positron) beam polarizations, P_{e^-} (P_{e^+}). The white region is accessible for $|P_{e^-}| \leq 85\%$, $|P_{e^+}| = 60\%$ [32].

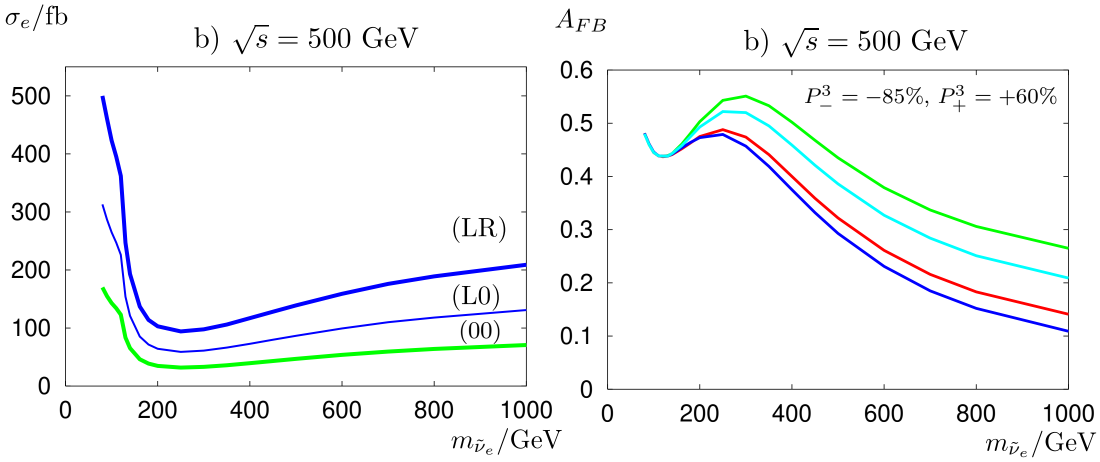

Figure 8: SUSY – Determination of the sneutrino mass $m_{\tilde{\nu}_e}$ in chargino production and decay: In a) the cross sections $\sigma \times BR$ in [fb] are given for different polarization configurations with $|P_{e^-}| = 80\%$, $|P_{e^+}| = 60\%$ and in b) the forward–backward asymmetry A_{FB} of the decay electron in $e^+e^- \to \tilde{\chi}_1^+\tilde{\chi}_1^-$, $\tilde{\chi}_1^+ \to \tilde{\chi}_1^0 e^- \bar{\nu}$ is shown for different masses of sneutrinos $m_{\tilde{\nu}}$ and selectrons $m_{\tilde{e}_L} = 130$ GeV, $m_{\tilde{e}_L} = 150$ GeV, $m_{\tilde{e}_L} = 200$ GeV and $m_{\tilde{e}_L}^2 = m_{\tilde{\nu}}^2 - m_W^2 \cos 2\beta$ (from top to bottom line) [32]. Other SUSY parameters as in the reference scenario.

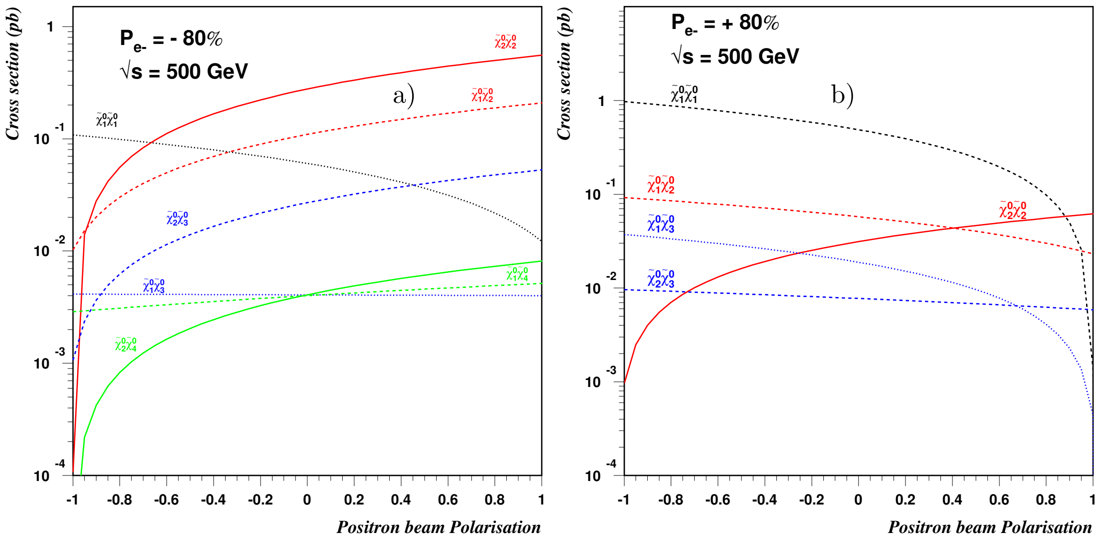

Figure 9: SUSY – Neutralino production: Cross sections for $e^+e^- \to \tilde{\chi}^0_i \tilde{\chi}^0_j$ [pb] at $\sqrt{s} = 500$ GeV in our reference scenario are shown for fixed electron polarization, in a) for $P_{e^-} = -80\%$ and in b) for $P_{e^-} = +80\%$, and variable positron polarization, P_{e^+} [30].

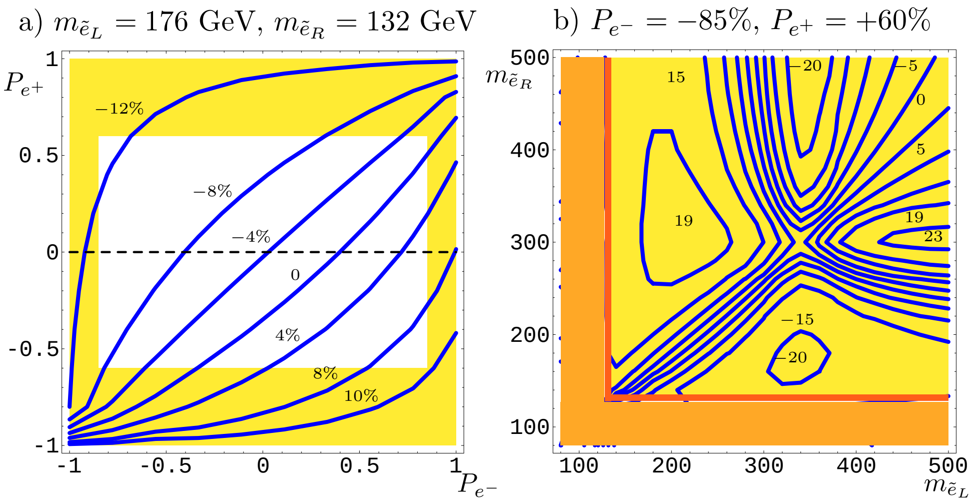

Figure 10: SUSY – Determination of the selectron masses $m_{\tilde{e}_{L,R}}$ in neutralino production and decay: Contour lines of the forward–backward asymmetry of the decay electron $A_{FB}/\%$ of $e^+e^- \to \tilde{\chi}^0_1\tilde{\chi}^0_2, \tilde{\chi}^0_2 \to \tilde{\chi}^0_1 e^+e^-$ at $\sqrt{s} = (m_{\tilde{\chi}^0_1} + m_{\tilde{\chi}^0_2}) + 30$ GeV in the reference scenario as a function of a) P_{e^-} and P_{e^+} for fixed $m_{\tilde{e}_L} = 176$ GeV, $m_{\tilde{e}_R} = 132$ GeV, and in b) $m_{\tilde{e}_L}$ and $m_{\tilde{e}_R}$ for fixed $P_{e^-} = -85\%$, $P_{e^+} = +60\%$. Outside the red coloured region direct production of $\tilde{e}_L$ or $\tilde{e}_R$ is not possible, $\sqrt{s}/2 < m_{\tilde{e}_{L,R}}$ [32].

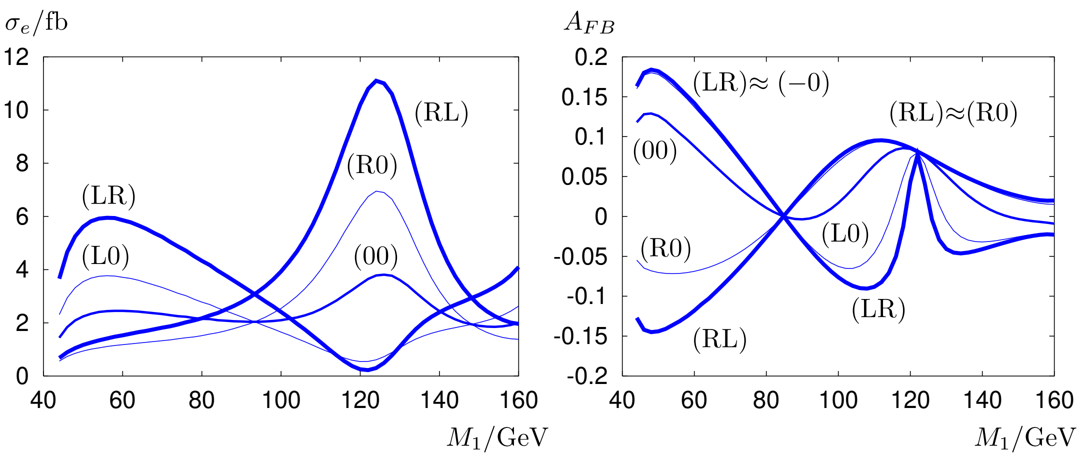

Figure 11: SUSY – Determination of M_1 parameter in neutralino production and decay: In a) cross sections $\sigma \times BR$ and in b) the forward–backward asymmetries A_{FB} of the decay electron of $e^+e^- \to \tilde{\chi}^0_1\tilde{\chi}^0_2$, $\tilde{\chi}^0_2 \to \tilde{\chi}^0_1 e^+e^-$ are shown at $\sqrt{s} = m_{\tilde{\chi}^0_1} + m_{\tilde{\chi}^0_2} + 30$ GeV as function of gaugino parameter M_1 for unpolarized beams (00), for only electron beam polarized (L0), (R0) with $P_{e^-} = \pm 85\%$ and for both beams polarized (LR), (RL) with $P_- = \mp 85\%$, $P_{e^+} = \pm 60\%$ [32]. Other SUSY parameters as in the reference scenario.

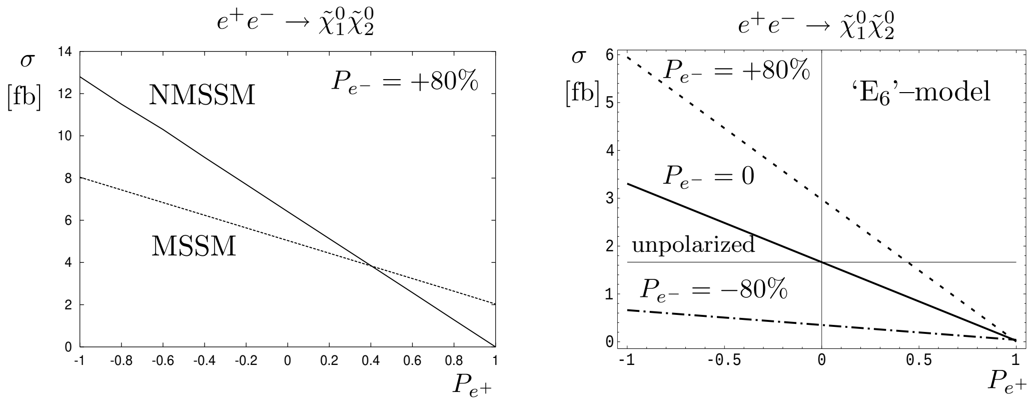

Figure 12: SUSY – Comparison of neutralino production in different SUSY models: Cross sections $e^+e^- \to \tilde{\chi}^0_1\tilde{\chi}^0_2$ in fb at $\sqrt{s} = 500$ GeV in a) in the NMSSM and MSSM for fixed electron polarization $P_{e-} = +80\%$ and in b) in the E_6–model for fixed $P_{e^-} = 0, \pm 80\%$ and variable positron polarization P_{e^+} [36].

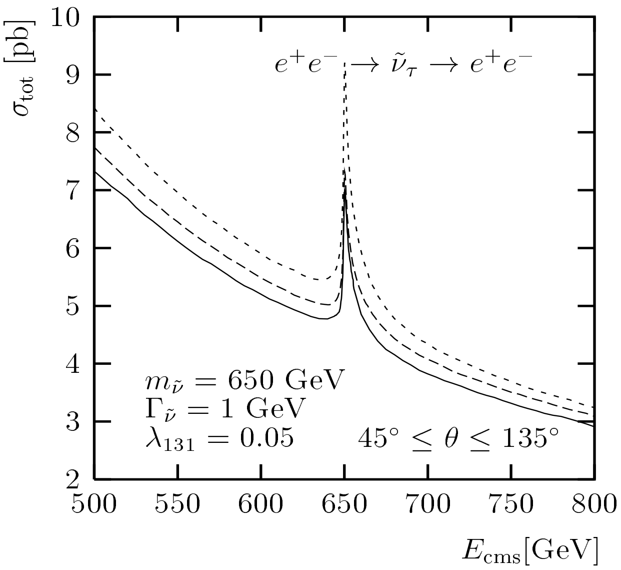

Figure 13: SUSY – Sneutrino production in R–parity violating model: Resonance production of $e^+e^- \to \tilde{\nu}$ interfering with Bhabha scattering for different configurations of beam polarization: unpolarized case (solid), $P_{e^-} = -80\%$ and unpolarized positrons (hatched) and $P_{e^-} = -80\%$ aand $P_{e^+} = -60\%$ (dotted) [37].